The seasonal evolution of NMHCs and light alkyl nitrates at middle to high northern latitudes during TOPSE

Nicola J. Blake,[1] Donald R. Blake,[1] Barkley C. Sive,[1,2] Aaron S. Katzenstein,[1] Simone Meinardi,[1] Oliver W. Wingenter,[3] Elliot L. Atlas,[4] Frank Flocke,[4] Brian A. Ridley,[4] and F. Sherwood Rowland[1]

Received 5 November 2001; revised 29 May 2002; accepted 30 May 2002; published 24 January 2003.

[1] The Tropospheric Ozone Production about the Spring Equinox (TOPSE) experiment was designed to follow the role of photochemistry in the evolution of the springtime maximum of tropospheric ozone (O_3) in the Northern Hemisphere (NH) at high latitudes. Determination of the composition and seasonal evolution of volatile organic carbon (VOC) species, which take part in and are good indicators for photochemical processes in the troposphere, was an important part of this study. We report measurements of a large number of C_2-C_{10} nonmethane hydrocarbons (NMHCs), selected C_1-C_2 halocarbons, and C_1-C_4 alkyl nitrates. These gases were quantified in whole air samples collected aboard the National Center for Atmospheric Research (NCAR) C-130 aircraft at altitudes between 30 m and 8 km. Seven TOPSE sampling trips were flown between early February and mid-May 2000 covering the region from Colorado (40°N) to Churchill (in Manitoba, Canada), Thule (in northern Greenland), and as far north as 85°N. These measurements represent the most comprehensive spatial characterization of the North American Arctic to date and revealed strong latitudinal, vertical, and temporal NMHC gradients. In the midtroposphere north of Churchill (58°N), ΣNMHCs decreased by ~6.2 ppbC between February and May (1.6 ppbC month^{-1}) and the magnitude of this change diminished with altitude. Over the same period, midtropospheric O_3 levels increased by ~16 ppbv (4.2 ppbv month^{-1}). Free tropospheric NMHC decreases were consistent with removal by hydroxyl (OH) radicals at an average mixing ratio for mid-March to mid-May of 4.1×10^5 mol cm^{-3}. The alkyl nitrates, which are a reservoir species for tropospheric reactive odd nitrogen (NO_Y), revealed similar latitudinal, vertical, and temporal gradients to their parent NMHCs. Their total decreased by ~4 pptv month^{-1}, representing 10% or less of NO_Y. In conjunction with meteorological trajectory analysis, different trace gas signatures provided significant clues to the origins of individual polluted air masses. Several of these air masses were rapidly advected over the Pole from source regions in northeastern and western Europe as well as an air mass that originated over the southwestern United States/Baja California that contained unusually high levels of alkanes. In addition, episodes of low boundary layer (BL) O_3 associated with low NMHC mixing ratios and trajectories from over the Arctic Ocean were frequently sampled toward the latter part of the experiment. The TOPSE data described here provide a unique picture of NH trace gas evolution from winter to summer that will be invaluable to models investigating the role that anthropogenic emissions play in high latitude O_3 chemistry. *INDEX TERMS:* 0322 Atmospheric Composition and Structure: Constituent sources and sinks; 0345 Atmospheric Composition and Structure: Pollution—urban and regional (0305); 0365 Atmospheric Composition and Structure: Troposphere—composition and chemistry; 0368 Atmospheric Composition and Structure: Troposphere—constituent transport and chemistry; *KEYWORDS:* Arctic troposphere, airborne measurements, seasonal cycle, NMHCs, alkyl nitrates, methyl nitrate

Citation: Blake, N. J., D. R. Blake, B. C. Sive, A. S. Katzenstein, S. Meinardi, O. W. Wingenter, E. L. Atlas, F. Flocke, B. A. Ridley, and F. S. Rowland, The seasonal evolution of NMHCs and light alkyl nitrates at middle to high northern latitudes during TOPSE, *J. Geophys. Res.*, *108*(D4), 8359, doi:10.1029/2001JD001467, 2003.

[1]Department of Chemistry, University of California, Irvine, Irvine, California, USA.

[2]Now at Climate Change Research Center, Institute for the Study of Earth, Oceans and Space, University of New Hampshire, Durham, North Carolina, USA.

[3]Department of Chemistry, New Mexico Institute of Mining and Technology, Socorro, New Mexico, USA.

[4]Atmospheric Chemistry Divison, National Center for Atmospheric Research (NCAR), Boulder, Colorado, USA.

0148-0227/03/2001JD001467$09.00

1. Introduction

[2] Volatile organic carbons (VOCs) provide fuel for ozone (O_3) production, and nitrogen oxides (NO_X = NO + NO_2) act as photochemical catalysts. Therefore, nonmethane hydrocarbons (NMHCs) are key species in the photochemical production of tropospheric O_3, and directly influence hydroxyl (OH) radical concentrations. Along with dynamic processes, photochemical oxidation dictates the rate at which the large variety of trace gases emitted from natural and anthropogenic sources are transformed.

[3] Springtime is a particularly interesting and challenging time to study how the atmosphere reacts to rapid changes of sunlight and temperature. During this period NMHC lifetimes change from several months to days, making the composition of VOCs particularly useful for evaluating radical sources and contributions to tropospheric O_3 production. Because of their importance to atmospheric photochemistry, airborne measurements of NMHCs over a wide range of altitudes, latitudes, and photochemical conditions were an essential component of the Tropospheric Ozone Production about the Spring Equinox (TOPSE) experiment.

[4] Previous atmospheric measurements indicate the buildup of a wide range of NMHCs in late winter to early spring in the lower, middle, and even in the upper Northern Hemisphere (NH) troposphere [e.g., *Singh and Salas*, 1982; *Hov et al.*, 1984; *Blake and Rowland*, 1986; *Anderson et al.*, 1993; *Penkett et al.*, 1993; *Blake et al.*, 1997]. This buildup appears to prime the atmospheric chemical system for a burst of photochemical oxidant production when insolation and temperatures increase, and circulation patterns change in early spring. Therefore, it may contribute to the spring maximum in O_3 that lags the maximum in NMHC by several months [e.g., *Penkett et al.*, 1993].

[5] The main sink for hydrocarbons and halocarbons with abstractable hydrogen atoms, denoted below as RH, is through oxidative reaction with OH radicals (·OH):

$$RH + \cdot OH \rightarrow R \cdot + H_2O \qquad (1)$$

Because the rate of (1) differs significantly among the various NMHCs, their tropospheric lifetimes vary widely. Relative mixing ratios of the different gases offer important information about their sources [e.g., *Blake et al.*, 1994] and can provide insight into photochemical processing and mixing [e.g., *McKeen et al.*, 1996; *Wingenter et al.*, 1996, 1999].

[6] Abundant sunlight and high humidity favor the photochemical production of OH, so its concentration varies diurnally, seasonally, and spatially. Minimum OH levels are found at high latitudes during winter, causing significantly reduced removal rates for many trace gases. The primary driving force for radical chemistry is photolysis of O_3 and the subsequent reaction of $O(^1D)$ and H_2O, which benefits not only from the increasing insolation but higher H_2O content of the warming air. Consequently, those gases with substantial emissions maintained throughout the year exhibit maximum background levels in late winter, with minimum levels occurring during late summer. This seasonal variation in boundary layer (BL) concentrations has been reported for many NMHCs and C_2Cl_4 [e.g., *Singh and Salas*, 1982; *Hov et al.*, 1984, 1991; *Blake and Rowland*, 1986; *Singh et al.*, 1988; *Lightman et al.*, 1990; *Penkett et al.*, 1993; *Jobson et al.*, 1994a; *Goldstein et al.*, 1995; *Wang et al.*, 1995; *Blake et al.*, 1997; *Gupta et al.*, 1998]. Relatively few seasonal airborne, or nonboundary layer, measurements have been made [*Ehhalt et al.*, 1985, 1991; *Lightman et al.*, 1990; *Anderson et al.*, 1993; *Penkett et al.*, 1993; *Blake et al.*, 1997].

[7] NMHCs are important precursors of secondary CH_2O, which is largely produced during the OH oxidation of hydrocarbons. The photolysis of CH_2O makes a particularly large contribution to HO_X sources during TOPSE [*Fried et al.*, 2002; *Wang et al.*, 2002]. Relative to the total HO_X source, CH_2O makes a larger contribution at higher altitudes and latitudes where the decrease of H_2O vapor concentrations with temperature reduces the source from the reaction $O(^1D)$ and H_2O.

[8] Many trace gases are entirely anthropogenic and are released predominantly in urban areas, so that their levels can be used to estimate recent anthropogenic influence on an air mass. Industrial activity is indicated by elevated concentrations of gases such as C_2Cl_4 [*Crutzen*, 1980; *Rasmussen et al.*, 1982; *Blake et al.*, 1994, 1996, 1997]. Natural gas emissions are associated with elevated levels of methane, ethane, and other light alkanes, with no accompanying halocarbons [*Blake et al.*, 1994]. Liquefied petroleum gas (LPG) leakage is likely the largest source of atmospheric propane and the butanes [*Blake and Rowland*, 1995], and petroleum refining activities emit mostly ethane, propane and other alkanes [*Sexton and Westberg*, 1979].

[9] Alkyl nitrates originate from both continental and marine sources [*Roberts*, 1990; *Atlas et al.*, 1993; *Ridley et al.*, 1997; *Blake et al.*, 1999, 2002]. Ocean waters are the principle source of methyl nitrate ($MeONO_2$) [*Blake et al.*, 2002]. The heavier alkyl nitrates ($>C_1$) are photochemically produced from the oxidation of parent hydrocarbons following the OH radical initiated oxidation of alkanes in the presence of NO_X [*Darnall et al.*, 1976; *Atkinson et al.*, 1982; *Roberts*, 1990]. The light alkyl nitrates ($<C_4$) are removed principally by photolysis, with OH reaction playing a progressively more important role as the hydrocarbon chain length increases [*Clemitshaw et al.*, 1997]. Alkyl nitrates have atmospheric lifetimes ranging from about 1 month to several days, depending on alkyl chain length, thus long-range transport plays an important role in their remote tropospheric distributions [*Atherton*, 1989; *Bertman et al.*, 1995]. Until recently, few alkyl nitrate measurements had been made, especially from aircraft [e.g., *Ridley et al.*, 1997; *Blake et al.*, 2002]. Marine measurements of alkyl nitrates and multifunctional alkyl nitrates have been recently summarized by *Fischer et al.* [2000]. They are an important class of atmospheric trace gases, in part because they have relatively low reactivity compared to other components of reactive odd nitrogen (NO_Y) so can serve as a reservoir for the long-range transport of nitrogen oxides (NO_X). As a result, alkyl nitrates have been of interest as a possible explanation of the lack of closure in the NO_Y budget [*Roberts et al.*, 1995, and references therein]. Alkyl nitrates can also be used as tracers of photochemical O_3 production from anthropogenic precursors [e.g., *Bertman et al.*, 1995; *Flocke et al.*, 1998; *Fischer et al.*, 2000].

[10] This paper presents the most spatially extensive measurements of the temporal trends in the composition of tropospheric NMHCs and light alkyl nitrates at high

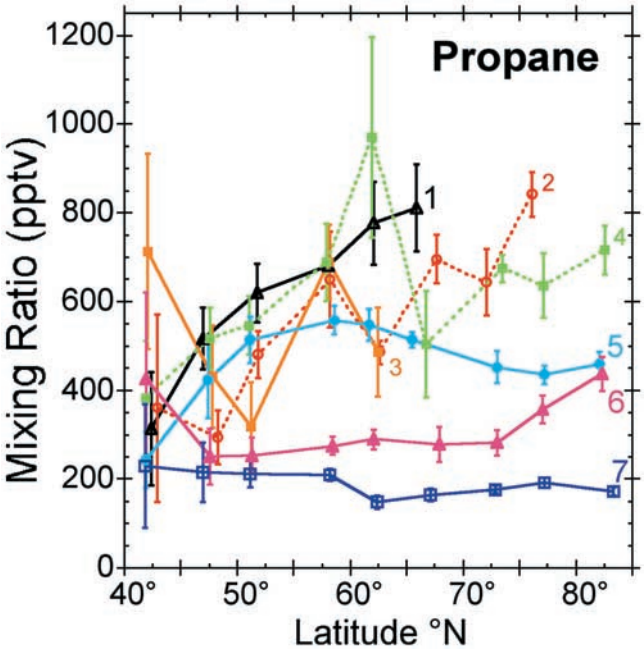

Figure 1. Latitude profile for propane. Each point is the mean value for a 5° latitude increment, altitudes 1–6 km, for each deployment (early February (1) to mid-May (7)). Error bars represent the 95% confidence level of the mean.

latitudes ever reported. The temporal trends in the composition of volatile organic trace gases provide significant clues to the origins of air masses in the TOPSE region. Since NMHCs and light alkyl nitrates have both natural and anthropogenic emission sources and a wide range of atmospheric lifetimes, these data will be invaluable to the global modeling community in validating emissions, photochemistry, and transport in 3-D models. All TOPSE data are archived in a standard format and are publicly available at http://topse.acd.ucar.edu/data/.

2. Experiment

[11] During TOPSE, we collected more than 2500 whole air samples in 2 L stainless steel canisters. Canisters were filled on the National Center for Atmospheric Research (NCAR) C-130 aircraft, transported to our home laboratory where the samples were assayed, and then the canisters were evacuated and sent back to the field. We sampled every 6–7 min during the horizontal flight legs, and every 1–3 min during selected vertical profiles, filling a maximum of 96 canisters per flight. During horizontal flight legs our sampling duration was usually adjusted to about 1 min, corresponding to an approximate sampling distance of 8 km. Typical vertical sampling distances were about 150 m.

[12] Details of the analytical procedures employed by the UCI laboratory are given by *Sive* [1998], *Colman et al.* [2001], and *Blake et al.* [2002] but are outlined as follows. For each sample 1520 ± 1 cm^3 (STP) of air was preconcentrated in a liquid nitrogen-cooled loop. This sample was directed to five different gas chromatographic column/detector combinations. Electron capture detectors (ECD, sensitive to halocarbons and alkyl nitrates), flame ionization detectors (FID, sensitive to hydrocarbons), and quadrupole mass spectrometers (MSD, for unambiguous compound identification and selected ion monitoring) were employed. The first column–detector combination (abbreviated as "DB5ms/MSD") was a DB5ms column (J&W; 60 m, 0.25 mm I.D., 0.5 μm film thickness) output to a MSD (HP-5973). The second combination ("DB1/FID") was a DB-1 column (J&W; 60 m, 0.32 mm I.D., 1 μm film thickness) output to a FID (HP-6890). The third combination ("PLOT-DB1/FID") was a PLOT column (J&W GS-Alumina; 30 m, 0.53 mm I.D.) connected in series to a DB-1 column (J&W; 5 m, 0.53 mm I.D., 1.5 μm film thickness) and output to an FID. The fourth combination ("Restek1701/ECD") was a RESTEK 1701 column (60 m, 0.25 mm I.D., 0.50 μm film thickness), which was output to an ECD. The fifth combination ("DB5-Restek1701/ECD") was a DB5 (J&W; 30 m, 0.25 mm I.D., 1 μm film thickness) column connected in series to a RESTEK 1701 column (5 m, 0.25 mm I.D., 0.5 μm film thickness) and output to an ECD. The DB5ms/MS, DB1/FID, PLOT-DB1/FID, Restek1701/ECD, and DB5-Restek1701/ECD combinations received 10.1%, 15.1%, 60.8%, 7.2%, and 6.8% of the sample flow, respectively.

[13] Our analytical accuracy ranges from 2% to 20%. The precision of the measurements varies by compound and by mixing ratio. For example, the measurement precision is 1% or 1.5 pptv (whichever is larger) for the alkanes and alkynes, and 3% or 3 pptv (whichever is larger) for the alkenes [*Sive*, 1998]. By comparison, the lines connecting the points in Figures 1 and 2 are approximately 5–20 pptv. The precision for the alkyl nitrates was better than 2% at the levels observed during TOPSE [*Colman et al.*, 2001]. The precision for C_2Cl_4 at 5 pptv is ±0.05 pptv [*Colman et al.*, 2001]. The limit of detection (LOD) is 3 pptv for the NMHCs. The alkyl nitrate detection limit was 0.02 pptv

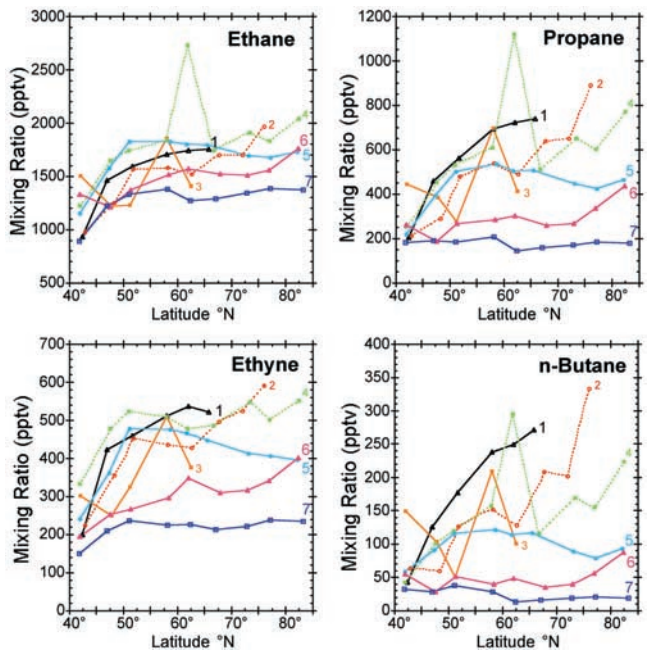

Figure 2. Latitude profiles for ethane, propane, ethyne, and *n*-butane. Each point is the median value for a 5° latitude increment, altitudes 1–6 km, for each deployment (early February (1) to mid-May (7)).

Table 1. Number of Samples per 5° Latitude Range for Each Deployment for the Altitude Range 1–6 km

	Latitude Range (°N)								
Deployment	40–45	45–50	50–55	55–60	60–65	65–70	70–75	75–80	80–85
1	28	43	49	37	27	25			
2	49	36	29	45	34	44	21	19	
3	27	33	20	26	22				
4	29	40	27	36	15	4	44	40	33
5	23	28	27	63	44	3	30	31	10
6	21	26	23	53	21	19	30	47	29
7	16	22	27	45	24	21	29	37	36

(except 0.01 pptv for methyl nitrate) [*Colman et al.*, 2001]. C_2Cl_4 was present at mixing ratios well above its detection limit at all times. The canister air was also analyzed for CO using GC with FID, as described by *Hurst* [1990] and *Lopez* [2002] using a packed column GC separation of CO followed by reduction to methane on a nickel catalyst and detection by FID. The absolute accuracy of the CO measurements calibrated against NIST standards was ±7%, with a DL of 5 ppbv [*Lopez*, 2002].

[14] TOPSE made experimental observations over a very wide range of environmental and dynamic conditions during the entire winter-to-spring transition. The altitude range of the NCAR C-130 flying laboratory was 30 m to 8 km. Sampling took place at approximately biweekly intervals from early February to mid-May 2000 in a series of 7 round trip deployments from Colorado (40°N) to Churchill, Canada (58°N); Thule (77°N) in northern Greenland; and as far north as 85°N (Atlas et al., The TOPSE experiment: Introduction, submitted to *Journal of Geophysical Research*, 2002, hereinafter referred to as Atlas et al., submitted manuscript, 2002). The trips were as follows: deployment 1, 4–9 February (Flights 5–8, Julian Days (JDays) 35–40); deployment 2, 21–27 February (Flights 9–13, JDays 52–58); deployment 3, 5–8 March (Flights 14–17, JDays 65–68); deployment 4, 19–26 March (Flights 18–23, JDays 79–86); deployment 5, 2–7 April (Flights 24–30, JDays 93–102); deployment 6, 23–30 April (Flights 31–36, JDays 114–121); and deployment 7, 15–23 May (Flights 37–42, JDays 136–144). Most of these deployments got far enough north to land at Thule, but deployments 1 and 3 were limited to local flights out of Churchill (Atlas et al., submitted manuscript, 2002).

3. Large-Scale Seasonal Evolution

3.1. Latitudinal Variation

[15] To get a "big picture" view of the seasonal evolution of trace gases during the 7 TOPSE deployments the mid-troposphere data (1–6 km) for each deployment are divided by latitude into 5° bins (BL concentration trends are discussed by B. C. Sive et al., (Non methane hydrocarbon and halocarbon measurements made over the Arctic and high northern latitudes: Impact of halogen chemistry on Arctic tower tropospheric ozone, submitted to *Journal of Geophysical Research*, 2002, hereinafter referred to as Sive et al., submitted manuscript, 2002). Table 1 shows that the number of samples in each latitude division varied between 3 and 63, with most bins containing at least 20 samples. The mixing ratio variability in each bin is indicated for propane in Figure 1 by error bars that represent the 95% confidence level of the mean, which is a useful quantity because it reflects both the variability of the measured air masses and the number of samples in each bin. For example, the large error bars for the deployment 4 data collected between 60°N and 70°N not only reflect the large variability in atmospheric mixing ratios encountered (see later), but also the relatively small number of samples collected in this region. Ideally we would include error bars for each gas, but unfortunately the plots look too crowded. In Figure 2, the median mixing ratios for each bin are plotted to reduce the impact of individual pollution plumes and stratospheric intrusions.

[16] In general, the NMHCs show a strong latitudinal gradient, with consistently lower median mixing ratios south of approximately 45°N for all gases (Figure 2). The rate of seasonal decrease in mixing ratios is proportional to OH reactivity, i.e., ethane, which is the longest-lived NMHC with a summer lifetime of about 70 days (much longer in winter) shows very little decrease until late in the project. In early April (deployment 5), ethane still manifested high mixing ratios at all latitudes north of about 50°N. The levels were reduced somewhat from early April to mid-May (deployment 7), but ethane maintained a slight latitudinal gradient, with higher northerly values. This is consistent with what we know from other projects [e.g., *Penkett et al.*, 1993; A. L. Swanson et al., Seasonality of C_2–C_4 NMHC and C_1–C_4 alkyl nitrates on the Arctic ice-sheet at Summit, Greenland, in review, 2002, hereinafter referred to as Swanson et al., in review, 2002], i.e., that long-lived ethane typically decreases relatively slowly in spring, and does not reach its summer minimum until August.

[17] Ethyne, the next longest-lived gas shown (summer lifetime ~18 days), also did not change significantly until after the early April trip (deployment 5), and its mixing ratios at the highest latitudes remained elevated into late April (deployment 6) (Figure 2). By contrast, levels of propane (summer lifetime ~13 days) decreased faster and were depleted over a wider latitude range by deployment 6. In fact, by the end of the TOPSE period the latitude gradient for propane became slightly negative, consistent with the strong midlatitude NH continental source of propane combined with a short summer lifetime relative to transport times to remote high latitudes.

[18] *n*-Butane is removed more rapidly at all latitudes and is reduced to quite low levels (compared with deployment 1) by early April (Figure 2). Its initially strong latitudinal gradient is almost gone by late April (deployment 6) except at the highest latitudes. By mid-May (deployment 7), *n*-butane mixing ratios also established a negative latitude gradient, with even lower median levels in the Arctic troposphere than near Colorado. This is because the Arctic region late in the spring is relatively remote, i.e., the travel time of air masses from midlatitude source regions is long compared to butane's summer atmospheric lifetime (about 5 days).

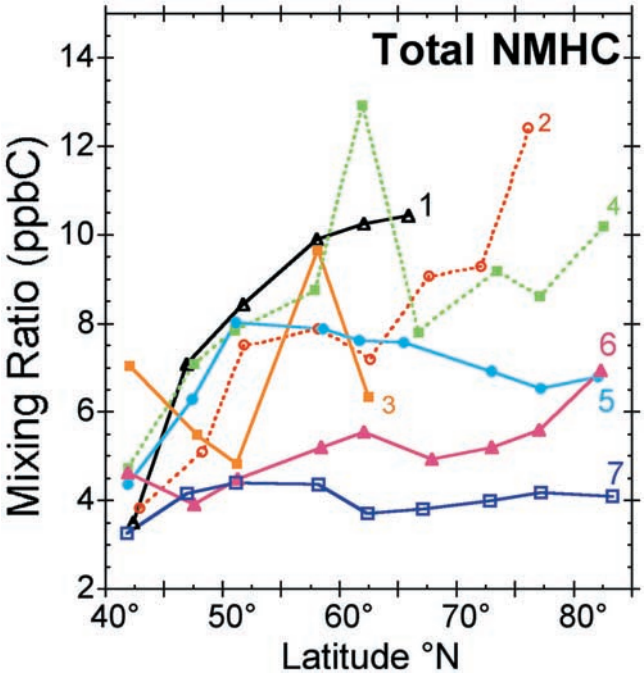

Figure 3. Same as Figure 2, but for total C_2-C_9 NMHCs.

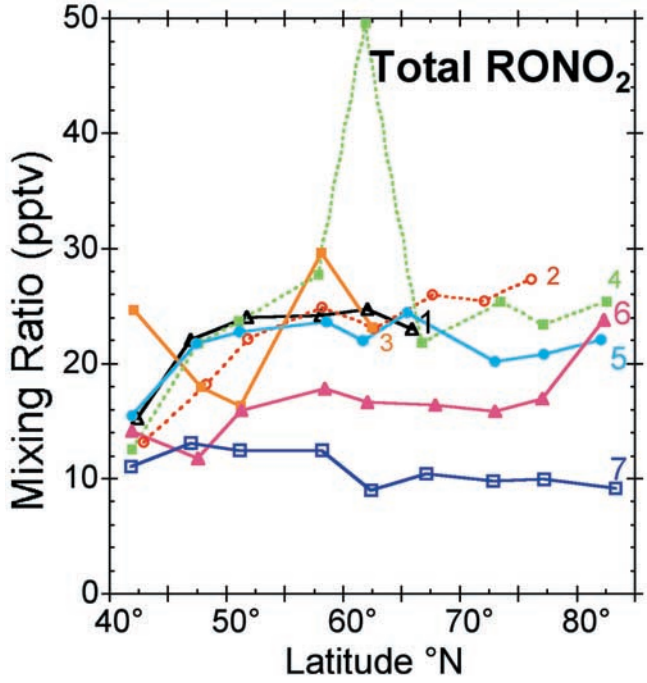

Figure 4. Same as Figure 2, but for total light (C_1-C_4) alkyl nitrates.

[19] The change in total carbon over all C_2-C_9 NMHCs (mixing ratio × number of carbons in molecule) between 1 and 6 km as a function of latitude illustrates the composite picture of the winter reactive carbon reservoir being gradually depleted further and further north (Figure 3). In general, highest concentrations were sampled in early February and gradually decreased as the season progressed. Median total NMHC levels at 60°–70°N decreased from about 10.5 to 4 ppbC over the TOPSE period, with the most rapid change (approx. 60% of the total) taking place between deployments 4 and 7.

[20] The sum of the light alkyl nitrates maintained remarkably constant levels and latitudinal gradient throughout deployments 1–5, with generally highest levels (about 25 pptv) to the north of 50°N (Figure 4). However, these levels were significantly diminished by deployment 6, and minimum mixing ratios (about 10 pptv at 60°–70°N) with a slightly negative latitudinal gradient were observed for deployment 7. This temporal change is comparable to that observed for propane and *n*-butane (Figure 2). The negative gradient is again consistent with the strong NH midlatitude continental source of the precursor NMHCs, combined with short summer lifetimes for the C_3 and C_4 alkyl nitrates (which are similar to their parent alkanes). 2-butyl nitrate (2-$C_4H_9ONO_2$) makes the largest contribution (diminishing from about 9 to about 1.5 pptv at 65°N) to the temporal mixing ratio change in total C_2-C_4 alkyl nitrates at high northern latitudes (Figure 5). By contrast, methyl nitrate changes very little (by about 1.5 pptv) and not significantly until the final deployment (Figure 5). This is in accord with the observations of Swanson et al. (in review, 2002) made atop the Greenland ice sheet. Although methyl nitrate has only weak continental sources (unlike the longer-chain alkyl nitrates VOC reactions are very inefficient secondary sources of methyl nitrate) [*Roberts et al.*, 1998; *Blake et al.*, 2002], this gas exhibits a negative latitudinal gradient during deployment 7 similar to that of the longer-chain alkyl nitrates (Figure 5).

[21] Back-trajectories for air sampled in the free troposphere during deployment 7 (Flight 37) at about 45°N over the northern central United States and containing a relatively high average mixing ratio of 3 pptv of methyl nitrate, indicate that the air was transported from near Hawaii during the previous 10 days (Figure 6). The equatorial

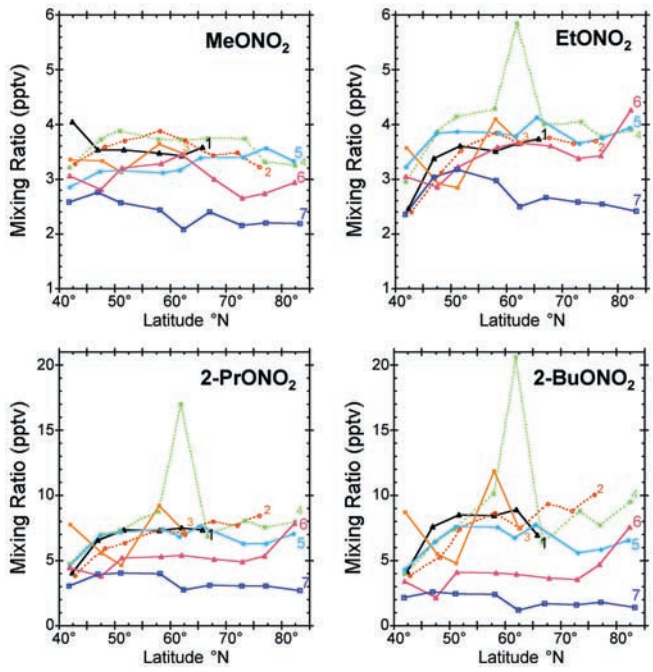

Figure 5. Same as for Figure 2, but for methyl nitrate, ethyl nitrate, 2-propyl nitrate, and 2-butyl nitrate.

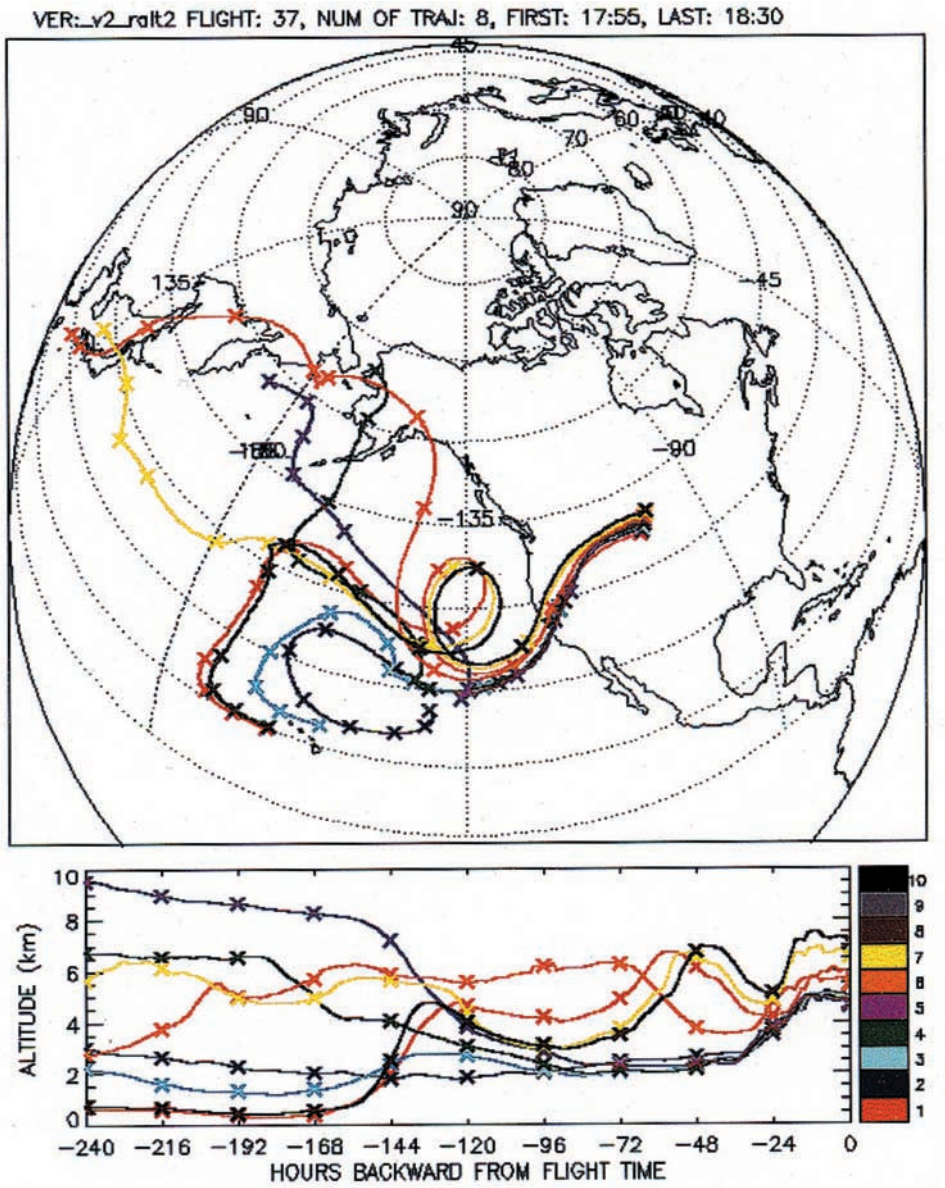

Figure 6. Back-trajectories for air arriving between 5 and 7 km at 45°N over the north central United States during Flight 37 (15 May 2000).

Pacific is known to be an important source of methyl nitrate [*Atlas et al.*, 1997; *Blake et al.*, 2002]. This air mass then traveled over populated areas of the western United States (Figure 6), where it could have been augmented with continental emissions of long-chain alkyl nitrate precursors. The tropical tropospheric lifetime of methyl nitrate is close to 1 month (longer at higher latitudes) so the molecule would easily survive the transit time over the Pacific and the western United States. Therefore, long-range transport from low latitudes is likely to account for the observed methyl and other alkyl nitrate gradients during deployment 7.

3.2. Vertical Trends

[22] The strong latitudinal gradients presented above, especially during the early part of the TOPSE period, prompted us to segregate out the low latitude samples for the following analysis of vertical trends. We arbitrarily chose to focus on the data to the north of Churchill (58°N) and further divided these data into 1 km altitudinal bins. Table 2 shows that the number of samples in each altitude division varied between 3 and 79, with most containing at least 10 samples. Deployment 3 has relatively few samples in each altitude division except for below 1000 m. This is reflected in the relatively large 95% confidence error bars for this deployment (except at low altitude) illustrated for propane in Figure 7.

[23] The early part of the TOPSE period (early February to mid-April) was characterized by strong vertical gradients for ethane, propane, ethyne, and *n*-butane north of 58° (Figure 8). The high mixing ratios at middle to low altitudes gradually diminished during TOPSE until the gradient was gone for all gases by mid-May. As with the latitudinal gradients described earlier (Figure 2), the vertical gradients disappeared faster for the shorter-lived gases such as propane and *n*-butane (Figure 8).

Table 2. Number of Samples Collected in 1000 m Altitude Intervals for Each Deployment for the Latitude Range 58°–85°N

	Altitude Range (m)							
Deployment	0–1000	1000–2000	2000–3000	3000–4000	4000–5000	5000–6000	6000–7000	7000–8000
1	25	12	12	15	11	23	3	
2	41	21	21	15	20	72	14	14
3	23	5	7	4	6	15	3	7
4	73	29	32	17	30	45	22	11
5	62	31	21	25	47	35	25	10
6	79	27	40	25	37	55	9	9
7	56	40	31	30	33	40	15	5

[24] Low median mixing ratios were observed below 1 km compared to the 1–2 km range for all four gases, ethane, propane, ethyne, and *n*-butane during deployments 4–6 (Figure 8). BL O_3 was also sharply lower below 1 km (Figure 9). Separate analysis of the NMHC and halocarbon data by Sive et al. (submitted manuscript, 2002) [see also *Ridley et al.*, 2002] reveal that these BL NMHC and O_3 losses are consistent with chlorine and bromine atom chemistry during the frequently encountered O_3 depletion events (ODEs), as reported previously for springtime Arctic studies [e.g., *Jobson et al.*, 1994b]. By contrast, median benzene mixing ratios were similar or higher in the BL for these same deployments (Figure 9). Benzene has relatively low reactivity with both Cl and Br radicals. For example, for OH oxidation, benzene's lifetime is about half that of ethyne, but ethyne reacts 20 times faster with Cl than benzene. Propane has a similar OH lifetime to that of benzene, but reacts nearly 40 times faster with Cl [*Atkinson et al.*, 1992]. In addition, ethyne reacts many times faster with Br radicals than benzene. This explains why benzene's vertical distribution (Figure 9) was relatively unaffected by the chemistry associated with ODEs.

[25] For low altitudes (1–3 km), total carbon contributed by the NMHCs gradually declined over the TOPSE period, from an average of approximately 15 ppbC in mid-February, to about 3.5 ppbC in mid-May (Figure 10). The upper tropospheric change (3–6 km) was much less pronounced, going from about 9.5 to about 4 ppbC during the same period. At the highest altitudes (above 6 km), very little change was observed for any NMHCs during the TOPSE period.

[26] The vertical gradients of total C_1–C_4 alkyl nitrates were less pronounced during the early deployments compared to those for total NMHCs (Figure 11). For example during deployment 2 (which was unaffected by any ODEs) there was a less than 20% drop between the median of total alkyl nitrates for the 0–1 km bin and that for the 5–6 km bin, compared to an approximately 45% decrease for total NMHCs (Figure 10). There was only a 35% drop for 2-butyl nitrate (Figure 12) compared to a nearly 70% drop for *n*-butane (Figure 8).

[27] The key to explaining the different vertical gradients for alkyl nitrates and their parent NMHCs lies in understanding the influence of air mass age combined with the

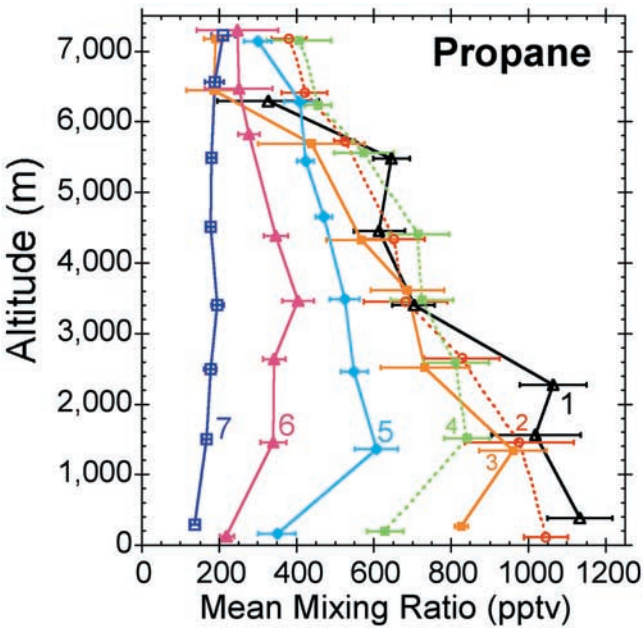

Figure 7. Seasonal evolution of the vertical distribution propane at high latitudes (58°–85°N) for each deployment (early February (1) to mid-May (7)). Each point is the mean value calculated for 1000 m altitude increments. Error bars represent the 95% confidence level of the mean.

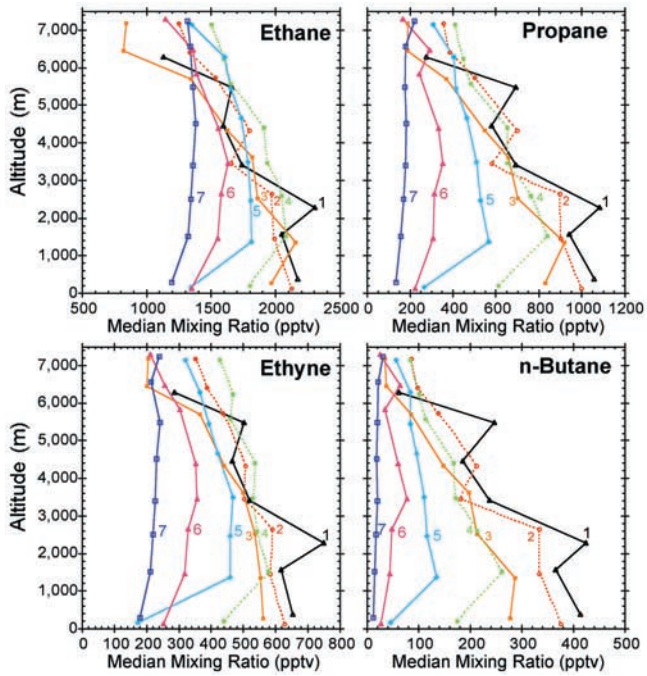

Figure 8. Vertical profiles for ethane, propane, ethyne, and *n*-butane. Each point is the median value for a 1000 m altitude increment, latitudes 58°–85°N, for each deployment (early February (1) to mid-May (7)).

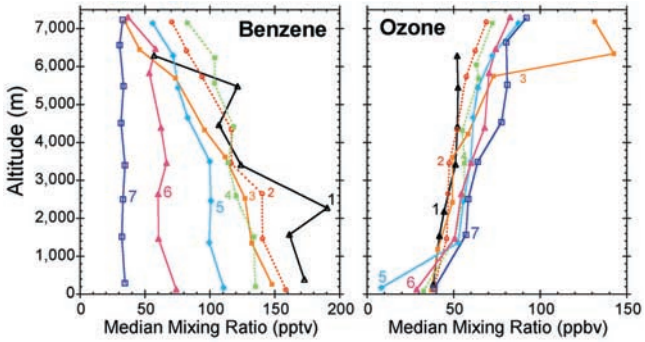

Figure 9. Same as for Figure 8, but for benzene and ozone.

long winter/spring Arctic lifetimes. A useful indicator of air mass age that has previously been used as an "index" against which to reference the atmospheric trends of the NMHCs and halocarbons is the ethyne/CO ratio [e.g., *Smyth et al.*, 1996; *Blake et al.*, 1997, 1999]. CO is relatively long-lived, with a similar lifetime to that of ethane. Atmospheric VOC oxidation contributes a significant secondary source of CO (40% over North America) [*Chin et al.*, 1994], but the principal source of both CO and ethyne in the NH is combustion, so typically they are tightly correlated. However, the different atmospheric lifetimes of the two gases mean that ethyne/CO ratios decrease with time compared to initial ratios near the source, or more accurately, with advancing "photochemical age" of an air mass. The long winter lifetime of both ethyne and CO explains the observation that ethyne/CO ratios in Figure 13 are close to values that are typical of initial emissions (approximately 4 pptv/ppbv) for deployment 1. The ratios tend to decrease with time, i.e., with increasing strength of sunlight and increasing temperatures as the troposphere is subject to increasing levels of OH (and therefore photochemical processing) (Merrill et al., Air mass origins during TOPSE, manuscript submitted to *Journal of Geophysical Research*, 2002). Over the TOPSE period, the lifetime of ethyne gradually decreases until the ethyne/CO ratio indicates well processed/photochemically aged air at all altitudes by the final (mid-May) deployment (7).

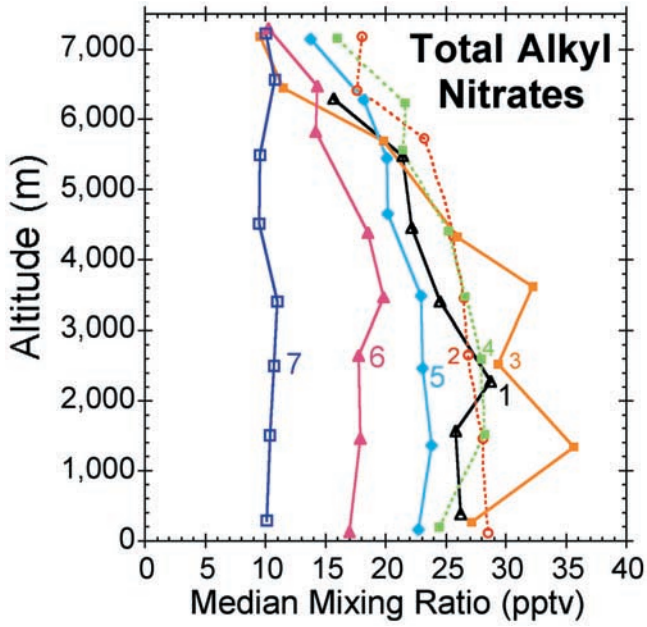

Figure 11. Same as for Figure 8, but for total light alkyl nitrates.

[28] In photochemical alkyl nitrate evolution, the ratio of a daughter alkyl nitrate to its parent hydrocarbon increases as an air mass ages because the daughter alkyl nitrate is produced at the expense of its parent hydrocarbon. For example, we can see from the ethyne/CO plot in Figure 13 that air in the 5–6 km bin during deployment 2 is (on average) relatively aged compared to that at 0–1 km. It

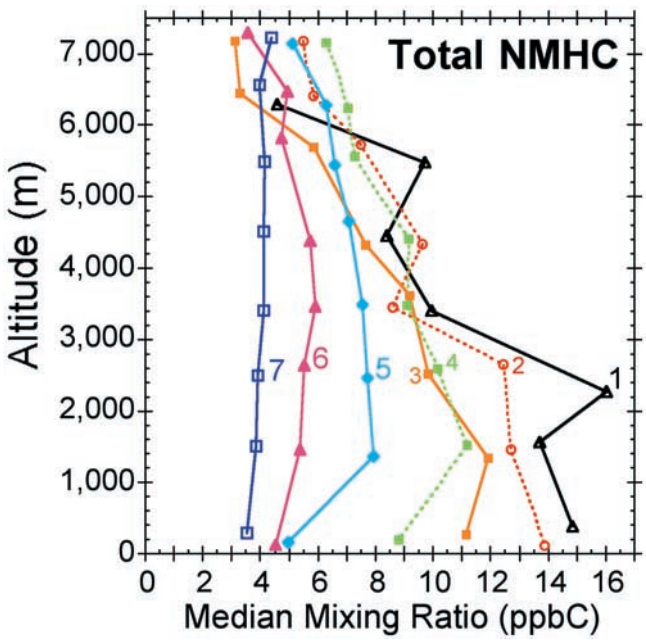

Figure 10. Same as for Figure 8, but for total NMHCs.

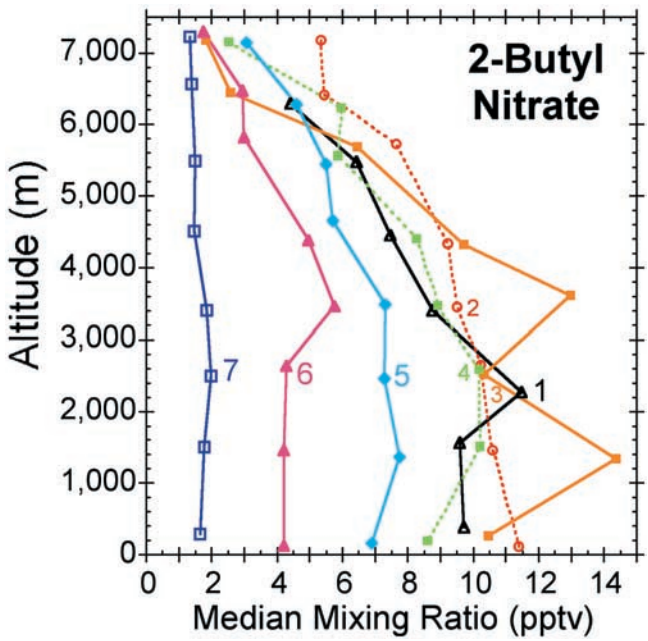

Figure 12. Same as for Figure 8, but for 2-butyl nitrate.

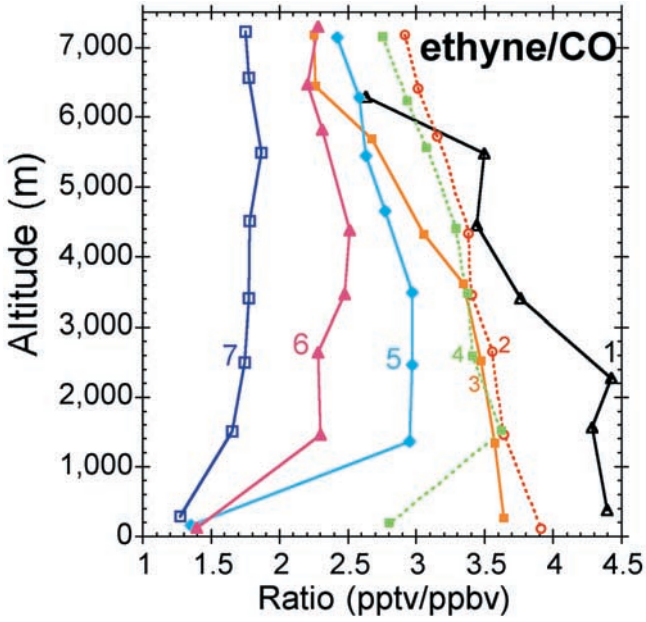

Figure 13. Same as for Figure 8, but for ethyne/CO.

follows that the ratio 2-butyl nitrate/*n*-butane (Figure 14) aloft is greater than at low altitude (0.055 compared to 0.03). Therefore, even though the levels of *n*-butane aloft are so much lower than at low altitude, the mixing ratios of the corresponding daughter alkyl nitrate fall off with altitude at a much slower rate. Following the same logic, 2-butyl nitrate/*n*-butane ratios at low altitudes during deployment 7 (Figure 14) are considerably enhanced because photochemical processing is occurring at a much faster pace in these relatively warm moist altitudes.

3.3. Temporal Trends

[29] Temporal trends north of 58° and between 1 and 6 km are shown in Figures 15, 16, and 17. These plots exclude data collected below 1 km (in order to avoid direct influence from ODEs) [*Ridley et al.*, 2002; Sive et al., submitted manuscript, 2002], as well as above 6 km (to reduce the direct impact of stratospheric air [*Browell et al.*, 2002; *Dibb et al.*, 2002]).

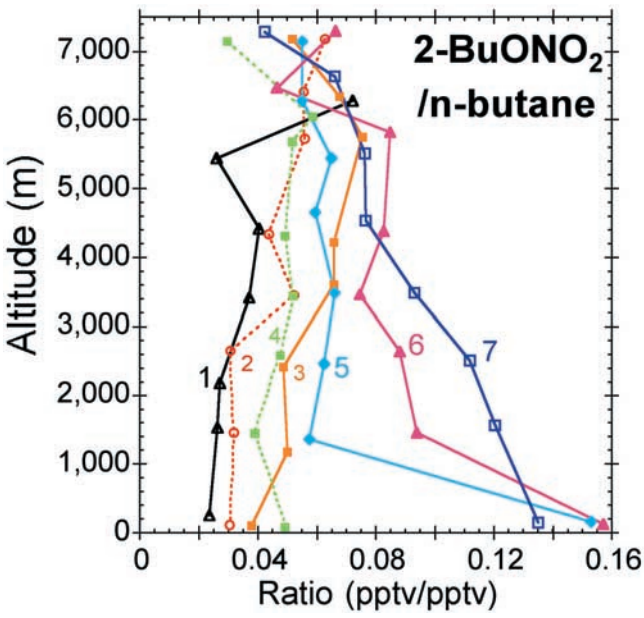

Figure 14. Same as for Figure 8, but for 2-butyl nitrate/*n*-butane.

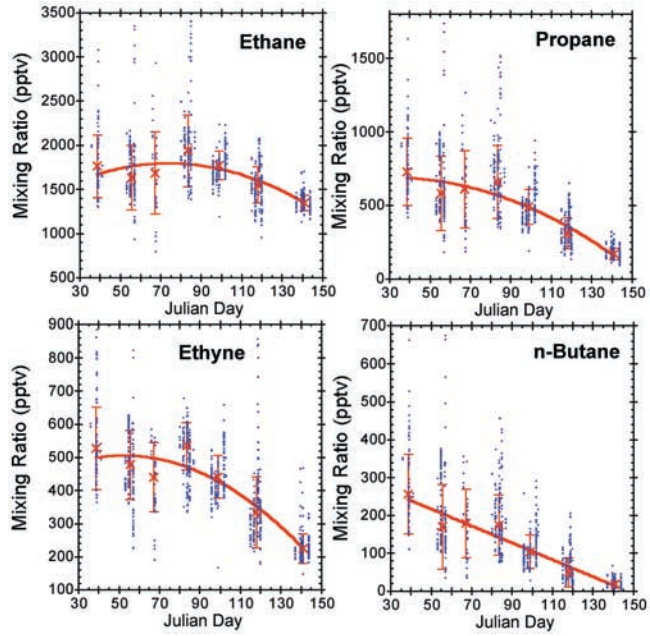

Figure 15. Temporal midtropospheric (1–6 km) trends at high latitudes (58°–85°N) for ethane, propane, ethyne, and *n*-butane. Individual samples are shown as dots. Crosses represent the median values for each of the 7 deployments. Error bars are ±1σ. The lines are polynomial fits to the median values and are shown as a guide.

[30] The average free tropospheric temporal trends in Figure 15 further illustrate that the rates of decrease of the C_2–C_4 NMHCs proceed in order of their OH lifetimes, with ethane declining at the slowest pace, and *n*-butane mixing ratios diminishing at a considerably faster rate. This point is investigated more fully below.

[31] Total NMHC mixing ratios decreased by ~6.2 ppbC (1.6 ppbC month^{-1}), while O_3 increased by ~16 ppb (4.2 ppbv month^{-1}) (Figure 16). Depending on conditions, roughly 1 ppb of carbon from the photochemical consumption of light NMHCs can produce 1 ppbv of O_3, provided that sufficient NO_X is available (see F. Flocke et al., Measure-

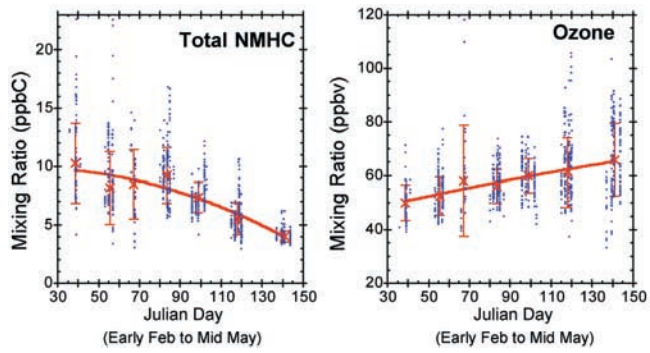

Figure 16. Same as for Figure 15, but for total NMHCs and ozone.

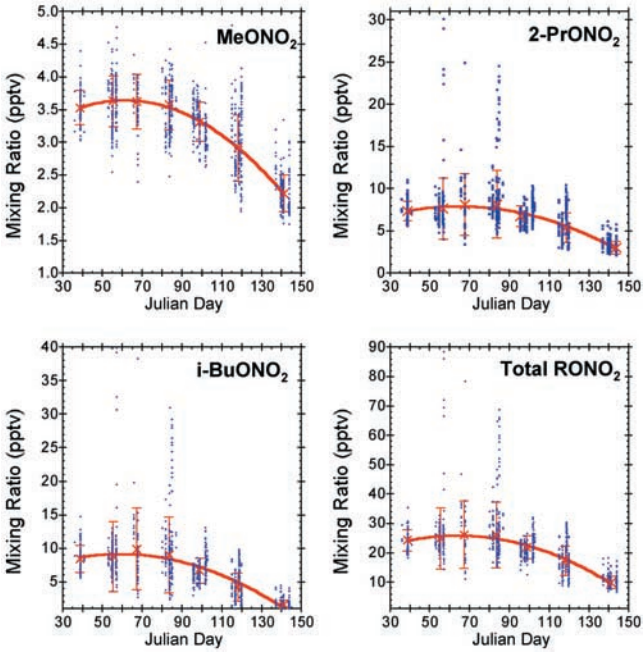

Figure 17. Same as Figure 15, but for methyl, 2-propyl, 2-butyl, and total (C_1-C_4) light alkyl nitrates.

ments of PAN and PPN, and the budget of reactive oxidized nitrogen during TOPSE, submitted to *Journal of Geophysical Research*, 2002, hereinafter referred to as Flocke et al, submitted manuscript, 2002). Therefore, in simplistic terms, this NMHC–O_3 comparison indicates that the processes associated with the spring photochemical NMHC consumption may be responsible for a substantial fraction of the O_3 increase between 1 and 6 km (see A. Klonecki et al., Seasonal changes in the transport of pollutants into the arctic troposphere: Model study, submitted to *Journal of Geophysical Research*, 2002, hereinafter referred to as Klonecki et al., submitted manuscript, 2002). Detailed analysis of tropospheric and stratospheric O_3 transport into the TOPSE region is presented by *Allen et al.* [2002], *Browell et al.* [2002], *Dibb et al.* [2002], and *Wang et al.* [2002].

[32] During the early part of the experiment, the individual NMHC variations with time show very little general trend, especially for the longest-lived gases such as ethane (Figure 15). In addition, the mixing ratio variations during this period tend to be larger for the first four deployments (to approximately JDay 90), as evidenced by the larger 1-SD error bars in Figure 15. *Jobson et al.* [1994b] also noticed more day-to-day fluctuations during the dark period at Alert (before 25 March). They attributed this observation to long-range advective transport of air masses with differing histories of exposure to sources into the region. This is plausible, considering that local OH levels before the spring equinox are so low [*Spivakovsky et al.*, 2000; *Mauldin et al.*, 2002] that relatively little oxidation is expected to occur between emission and sampling.

[33] Plots of the ratios of ethyne/CO and ethyne/benzene versus JDay shown in Figure 18 both illustrate the influence of chemical aging on the free tropospheric air masses over time. They confirm that chemical aging is very slow for the first 3 deployments (to approximately JDay 75) but becomes more rapid after the spring equinox, i.e., during the final three deployments.

[34] As we saw earlier with the vertical distributions, average levels of the alkyl nitrates 2-propyl nitrate (2-$C_3H_9ONO_2$) and 2-butyl nitrate start to decline later than their parent hydrocarbons propane and *n*-butane (Figures 17 and 15). They also tend to peak later in the winter, however, once they start to diminish their rate of decline is quite fast and follows the same trend as the NMHCs where the shortest-lived species decline at the fastest rate.

[35] Because the longer-chain alkyl nitrates are secondary products of HC oxidation, it follows that any oxidation of propane and *n*-butane that does occur over the winter period will contribute to increased levels of 2-propyl nitrate and 2-butyl nitrate. However, when the rate of photochemical reactions starts to increase rapidly after the spring equinox, the balance of photochemical production and loss is tipped in favor of net alkyl nitrate destruction. Then, due to their shorter photochemical lifetimes (relative to the shorter-chain alkyl nitrates), 2-propyl nitrate and 2-butyl nitrate decay rapidly.

[36] Levels of total light (C_1-C_4) alkyl nitrates peaked at an average of about 26 pptv (Figure 17). This total was dominated by 2-propyl nitrate and 2-butyl nitrate, which at 8 and 9 pptv, respectively each contributed about one third (Figure 17). The winter dominance of C_3-C_4 alkyl nitrates compares well with previously published surface data. During the 1992 Alert campaign (PSE92) in northern Canada, *Muthuramu et al.* [1994] measured nearly 35 pptv

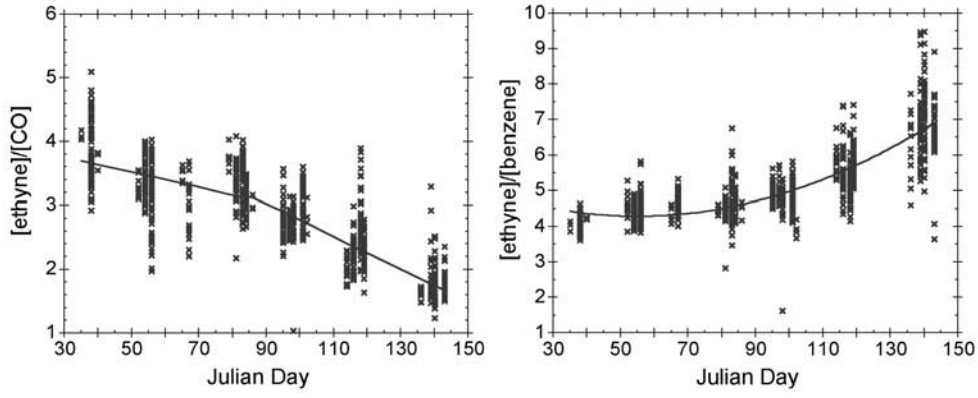

Figure 18. Trend of the ratios of ethyne/CO and ethyne/benzene versus JDay for latitudes 58°–85°N.

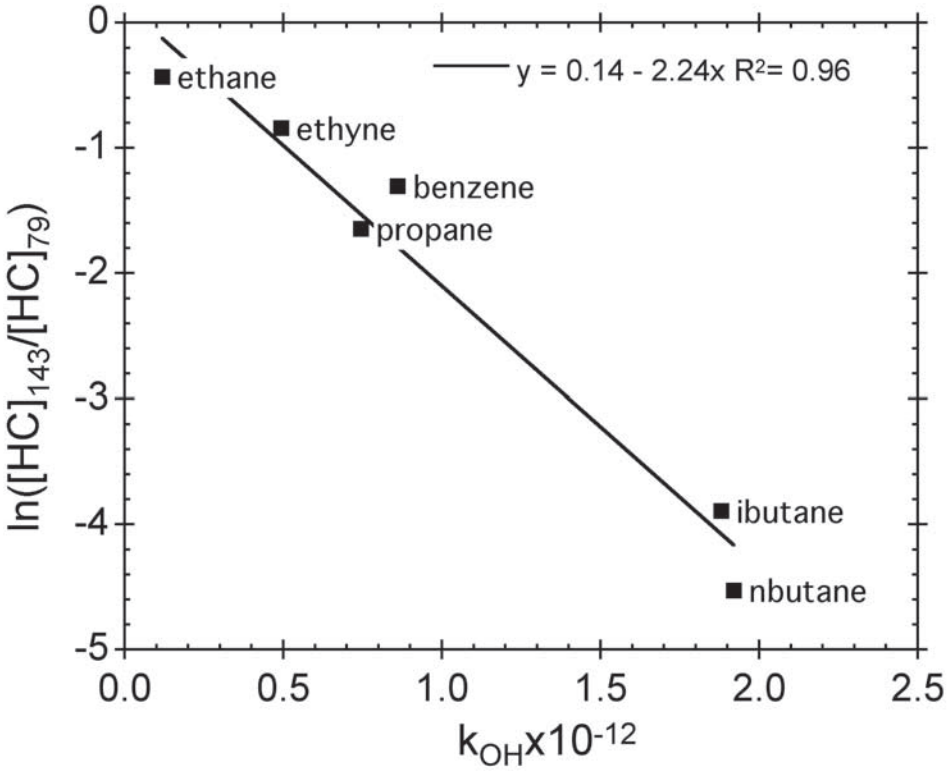

Figure 19. Correlation between hydrocarbon concentration change over the period JDays 79–143 (deployments 4–7) and hydroxyl rate constant at 243 K). Slope = $-\int$[OH]dt. Average [OH] calculated from this slope = 4.1×10^5.

total of C_3 and C_4 alkyl nitrates during peak winter concentrations, totaling roughly 50% of the light organic nitrate contribution. Swanson et al. (in review, 2002) measured peak C_1–C_4 alkyl nitrate levels between 30 and 42 pptv at Summit, Greenland, with 2-propyl nitrate and 2-butyl nitrate, comprising about 60% of the total.

[37] Total C_1–C_4 alkyl nitrates decreased by approximately 16 pptv during the latter part of TOPSE (JDays 83–142) (Figure 17) compared with a corresponding increase of about 50 pptv for NO_Y [Flocke et al., submitted manuscript, 2002; *Ridley et al.*, 2002]. As a result, the contribution of alkyl nitrates to NO_Y decreased from about 12% to only 3% from late March to late May. We note that tertiary nitrates (and multifunctional nitrates) are not measured with this technique, so the reported alkyl nitrate sum is a lower limit (by perhaps 20–30%) [e.g., *Fischer et al.*, 2000].

3.4. Estimation of Average OH

[38] Wintertime Arctic horizontal circulation is more vigorous, with many 10-day back-trajectories reaching back to Asia or Europe [e.g., *Kahl et al.*, 1997]. Summertime trajectories tend to be shorter as the Arctic air mass shrinks back to the north of most major pollution sources in North America and Eurasia. Thus, we would expect lower mixing ratios of NMHCs in summer due to much weaker transport from source regions alone, as demonstrated by the analysis of Klonecki et al. (submitted manuscript, 2002), whose chemical transport model uses hypothetical short-lived and long-lived tracers to mimic the spring decrease in the NMHCs. However, the strong seasonal trends within the source regions themselves [e.g., *Goldstein et al.*, 1995; *Hagerman et al.*, 1997; *Sharma et al.*, 2000], indicate that the winter–spring buildup at high latitudes is not solely a result of transport, but also a consequence of increased summertime photochemistry.

[39] In order to examine influences affecting seasonal variations of the NMHCs during TOPSE, we have applied an analysis using hydrocarbon ratios in a manner similar to that used previously by *Rudolph and Johnen* [1990] and *Jobson et al.* [1994b]. The analysis is based on the assumption that the changing ratios of the concentrations of hydrocarbon species can be used to characterize the average photochemical exposure of an air mass over time. This requires that the species be removed by photochemical reactions that follow second-order or pseudo-second-order (ethyne) kinetics as follows:

$$[HC]_f = [HC]_i \exp\left(-k_{HC}[OH]_{ave}t\right) \quad (2)$$

where $[HC]_i$ and $[HC]_f$ are the initial and final hydrocarbon (HC) concentrations, respectively, k_{OH} is the bimolecular rate constant for reaction of the hydrocarbon with OH, $[OH]_{ave}$ is the time averaged OH concentration, and t is the time between initial and final HC measurements. Dilution by nonnegligible concentrations of the longer-lived species will bias the determination of age as has been shown by *Mckeen and Liu* [1993]. However, the calculation still offers useful insight into the NMHCs removal processes when several different gases with a range of chemical lifetimes are employed.

[40] In Figure 19, the natural log of the ratio of hydrocarbon concentrations over the period JDays 79–143

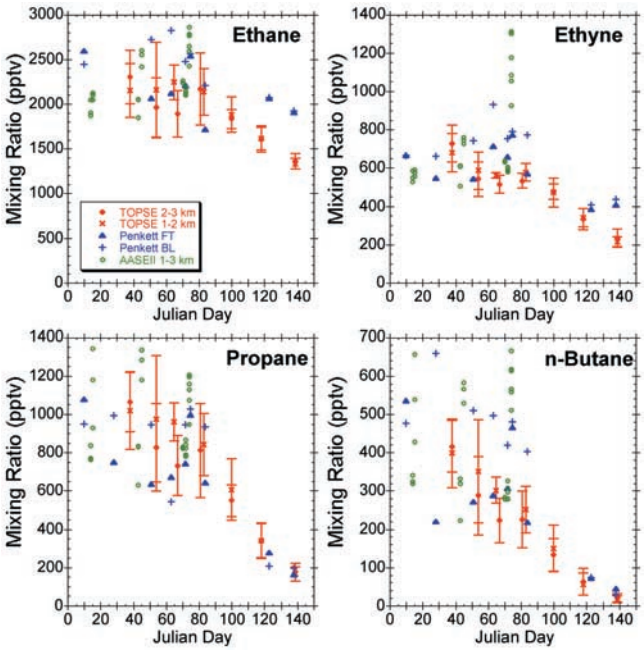

Figure 20. Comparison between TOPSE data (mean ± 1 SD) north of 58°N and in the altitude ranges 2–3 and 1–2 km data collected over the North Atlantic in the Free Troposphere (FT, <3 km) and the Boundary Layer (BL, <150 m) [*Penkett et al.*, 1993] and measurements made to the north of 58°N and between 1 and 3 km during AASEII [*Anderson et al.*, 1993].

(deployments 4–7) for the free troposphere (1–6 km) is plotted versus the OH rate constant (at 243 K) for each of the six HCs whose lifetime was long enough to be present at mean mixing ratios above their detection limit. Equation (2) can be manipulated to show that the slope of this plot represents $-\int[OH]dt$. The resulting correlation between the six HCs is very strong, indicating that OH chemistry dominated the seasonally decreasing NMHC levels. Average [OH] over the period JDays 79–143 calculated from this plot is 4.1×10^5 mol cm^{-3}.

[41] This OH calculation is not meant to imply that photochemical loss of NMHCs occurred in a single air mass that was located over the Arctic during the entire late March to late May period. Rather, this loss is likely the combined influence of local OH removal plus dilution with photochemically aged air masses from further south. The calculated value of OH is remarkably similar to that obtained by the model calculations of *Wang et al.* [2002], which were constrained by measured peroxide values. *Wang et al.* [2002] found that photochemical activity, as measured by sources of HO_X, increased rapidly at middle and high latitudes and that photolysis of CH_2O (a secondary product NMHC oxidation) makes a particularly large contribution to HO_X during TOPSE. They also found that relative to the total HO_X source, CH_2O makes a larger contribution at higher altitudes and latitudes where H_2O vapor concentrations are low.

4. Comparison With Previous Work

[42] Our results are in general agreement with surface seasonal NMHC studies reported by *Blake and Rowland* [1986], *Jobson et al.* [1994a], *Goldstein et al.* [1995], and *Swanson et al*. [2002]. In Figure 20 we directly compare our lower altitude results with aircraft-borne measurements reported by *Penkett et al.* [1993] and by *Anderson et al.* [1993]. Penkett et al. collected samples over the North Atlantic, north of the Arctic Polar front up to altitudes of about 3 km in 1988–1989. Anderson et al. reported measurements made during late winter 1992 as part of the Airborne Arctic Stratospheric Expedition (AASE II) campaign. The results agree remarkably well, indicating similar ethane levels and a relatively wide mixing ratio range during the period before the summer equinox, over a large portion of the NH. The Penkett et al. BL data tend to be at the high end of the free tropospheric TOPSE data during the early period to approximately JDay 80 (corresponding to deployment 4). This is consistent with the initially strong then diminishing vertical NMHC gradient discussed above. The comparison (Figure 20) also suggests that there has been no significant large-scale temporal trend for light NMHCs at high northern latitudes during the past decade.

[43] Our alkyl nitrate results compare well with measurements made at Alert [*Muthuramu et al.*, 1994] and on the Greenland ice sheet [Swanson et al., in review, 2002]. Early April total C_2–C_6 alkyl nitrate mixing ratios at a surface site in interior Alaska [*Beine et al.*, 1996] were approximately 15 pptv higher than reported here (Figure 17), but were similar by mid-May. The contribution from the C_5 and C_6 alkyl nitrates, which can be quite large in winter [*Muthuramu et al.*, 1994] but decay at a fast rate during the winter–spring transition, accounts for much of this early spring difference.

5. Case Studies

5.1. Flight 22 (Deployment 4)

[44] The previous sections have shown the large-scale changes encountered during the course of the TOPSE experiment. However, there is also a wealth of information to be obtained by scrutinizing the details of the many individual flights. Companion papers by Sive et al., (submitted manuscript, 2002), *Ridley et al.* [2002], and others document individual flights focused on such features as BL ODEs during TOPSE.

[45] Even employing median values, Figure 2 (and others) reveals evidence for individual pollution plumes. The most obvious example is observed in deployment 4 between 60°N and 65°N (Figure 2), where ethane, propane, and *n*-butane mixing ratios are elevated as the result of very high mixing ratios encountered on Flight 22. By contrast, ethyne levels were not unusually high. We have also chosen this flight to illustrate the power of combining our trace gas analysis with meteorological back-trajectory analysis. Figure 21 displays the mixing ratios of selected NMHCs, methyl nitrate and 2-butyl nitrate during Flight 22, which flew south from Thule to Churchill on 24 March. Two air masses with very different trace gas composition were encountered in the midtroposphere (approximately 2–6 km) and are highlighted in Figure 21 as a and b.

[46] Very high levels of ethane and propane were observed over the western shore of Hudson Bay (Figure 21, air mass b), and were accompanied by elevated levels of *n*-butane (not shown). This chemical signature is similar to that observed for cities such as Mexico City, which has

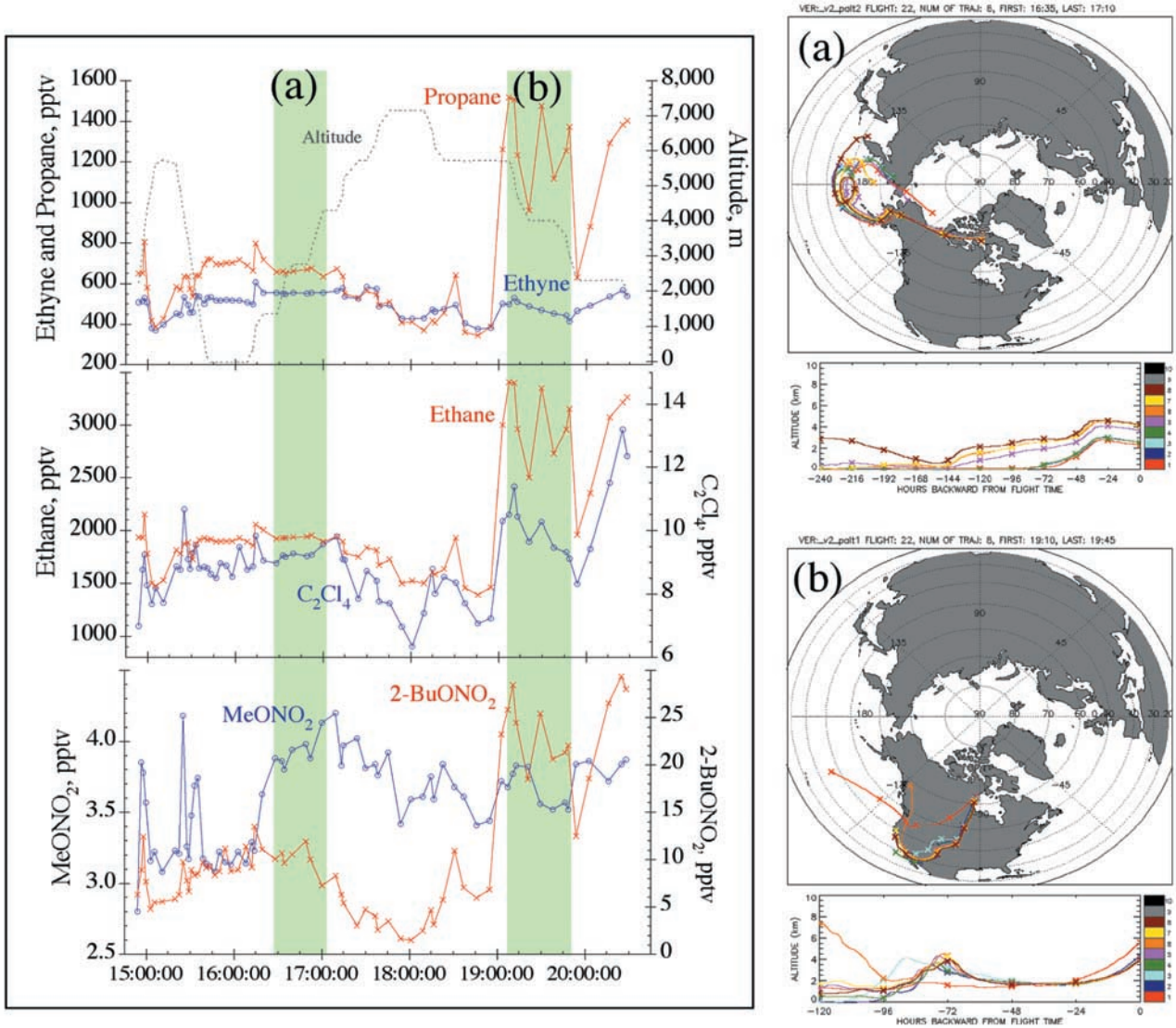

Figure 21. Altitude, propane, ethyne, ethane, C_2Cl_4, methyl nitrate, and 2-butyl nitrate versus time for Flight 22, Thule to Churchill, 24 March 2000 (deployment 4). Also shown are back-trajectories showing the origins of the air masses sampled during the highlighted sections (a) and (b) of the flight.

high LPG usage, but surprisingly, the combustion tracers such as ethyne remained very close to background levels, not what would be expected for a mixed urban plume. This indicates an origin associated more closely with oil/gas production [*Sexton and Westberg*, 1979; *Blake et al.*, 1992]. Consistent with this, 5-day back-trajectories for air mass (b) originate at low altitude over SW coastal United States/Baja California, the location of both natural gas and oil fields.

[47] High levels of 2-butyl nitrate (Figure 21) suggest that air mass b had been subject to significant photochemical processing in order to have produced so much of this secondary alkyl nitrate from its parent hydrocarbon. Because measured OH levels (and thus photochemical processing) were low in the Arctic during deployment 4 [*Mauldin et al.*, 2002], most of the *n*-butane is likely to have been added close to the southerly origin of air mass b (Figure 21), where photochemistry would be active.

[48] If we contrast this plume with the mixing ratio signature from a similar altitude range earlier in the flight (Figure 21, air mass a), we find much lower levels of ethane and propane. Ethyne and benzene (not shown) are again close to background levels, but there is a slight enhancement in methyl nitrate. Ethyl nitrate (not shown) is slightly elevated, but 2-butyl nitrate is not. The back-trajectories for this small section of the flight show that the air masses have circulated over the North Pacific, including a period at low altitude, near 40°N for the past 10 days or so. Therefore, the methyl nitrate (and ethyl nitrate) is likely to reflect a small contribution from ocean sources.

[49] We note that the back-trajectories shown for Flight 22 are not meant to be representative of the TOPSE period (or of TOPSE as a whole). They instead represent some of the diverse conditions that were sampled. In fact, air masses that had been advected across the Arctic Ocean were more typical of the TOPSE period. Indeed, model analysis

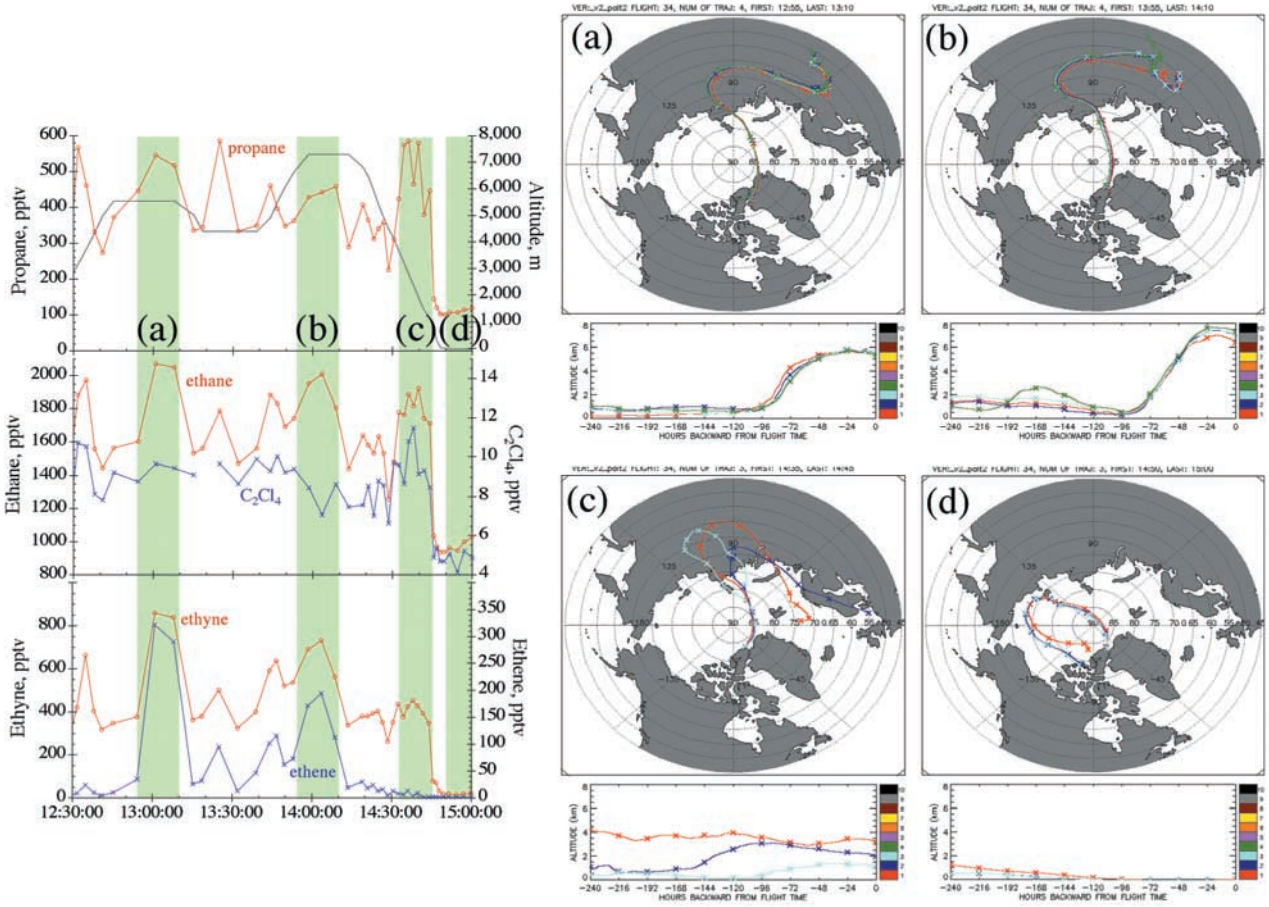

Figure 22. Altitude (gray line), propane, ethane, C_2Cl_4, ethyne, and ethene versus time for part of Flight 34, Thule-Thule, 27 April 2001. Four flight sections a, b, c, and d are highlighted and the trajectory plots for each of these sections are shown.

suggests that there was greater influence from the European continent than North America [*Merrill et al.*, 2002].

5.2. Flight 34 (Deployment 6)

[50] Flight 34 (north from Thule on 27 April 2000) was chosen to illustrate further the range of air mass transport conditions that contributed to the trace gas trends observed during TOPSE, including air masses advected across the Arctic Ocean and exhibiting influence from the European continent.

[51] The first two highlighted sections of the flight were sampled exactly 1 hour apart and at 5.5 and 7.5 km altitude, respectively (Figure 22, air masses a and b). Both are characterized by high levels of the reactive combustion tracer ethene, as well as by enhancements in the other combustion and fossil fuel-related NMHCs ethyne, ethane, and propane. The fact that the industrial tracer C_2Cl_4 is not elevated in either plume indicates that they originate from nonindustrial combustion sources such as biomass fires or vehicle traffic. The trajectories for both plumes (Figure 22, trajectories a and b) have similar low altitude origins over northeastern Europe from where they were transported within about 4 days, consistent with maintaining high levels of reactive ethene so late in the campaign. In fact, fast air mass transit clear across the Arctic Ocean occurred in less than 2 days.

[52] The third plume, sampled between 4 and 1 km was very different in chemical character, with low ethene and ethyne but relatively high C_2Cl_4, as well as ethane and propane (Figure 22, air mass c). The elevated C_2Cl_4 is consistent with trajectories that originate closer to industrialized western Europe (Figure 22, trajectory c). The high propane and ethane suggest that the air may have mixed with emissions from oil refining operations.

[53] The fourth highlighted section of the flight was sampled at low altitude in the Arctic BL. It is very different again but typical of many air masses that were sampled during deployments 4–7. This air mass is characterized by very low mixing ratios of all trace gases shown (Figure 22, air mass d). The trajectories remained at low altitude over the Arctic Ocean for at least the past 10 days (Figure 22, trajectory d). The very low O_3 associated with this air mass makes it one of the ODEs that are studied in depth in several companion papers [*Ridley et al.*, 2002; Sive et al., submitted manuscript, 2002].

6. Summary

[54] Strong latitudinal, vertical, and temporal gradients were observed for NMHCs and alkyl nitrates as part of the most comprehensive airborne survey of the Arctic troposphere accomplished to date. The low altitude measure-

ments compared well with previous work. We note that the mixing ratios of most gases were quite different near the surface from that in the free troposphere, so measurements over a wide altitude range are important for understanding their behavior at middle and high latitudes.

[55] Vertical and latitudinal gradients of all the measured NMHCs and alkyl nitrates diminished as photochemistry and dynamics increased during the winter–spring transition, in contrast to the observed increase in O_3 and NO_Y concentrations. The incidence (and sampling) of ODEs resulted in low median mixing ratios for ethane, propane, ethyne, and *n*-butane below 1 km.

[56] Over the TOPSE period, the winter reactive carbon reservoir was gradually depleted further and further north. In the northern part of the study region (>58°N) and between 1 and 6 km, median total NMHC levels decreased by ~6.5 ppbC from approximately 10.5 to 4 ppbC. Most of this loss occurred after the spring equinox, with the most rapid change (approx. 60% of the total) taking place between late March and late May. The upper tropospheric decrease (3–6 km) was much less pronounced, falling from about 9.5 to about 4 ppbC during the entire TOPSE period. At the highest altitudes (above 6 km), very little change was observed for any NMHC.

[57] The rates of decrease observed for a suite of individual NMHCs over the late March to late May period were in accord with their OH radical reaction rates, implying primary removal by OH rather than different source types, being principally responsible for the observed seasonal NMHC trends. Further, they were consistent with the sampled air having been exposed to average OH levels equivalent to 4.1×10^5 mol cm^{-3}.

[58] Total C_1–C_4 alkyl nitrates decreased by approximately 16 pptv during the latter part of TOPSE. 2-butyl nitrate makes the largest contribution (diminishing from about 9 to about 1.5 pptv at 65°N) to the temporal mixing ratio change in total alkyl nitrates at high northern latitudes. By contrast, methyl nitrate changes very little (by about 1.5 pptv) Average levels of the alkyl nitrates 2-propyl nitrate and 2-butyl nitrate peak later in the winter so start to decline later than their parent hydrocarbons. However, once they start to diminish their rate of decline is quite fast and in order of their atmospheric lifetimes.

[59] Several examples of long-range transport of plumes with different trace gas signatures from sources that influenced the Arctic troposphere during TOPSE were illustrated.

[60] **Acknowledgments.** We are very grateful for the excellent support from our colleagues at UC Irvine during the project, especially Murray McEachern, Kevin Gervais, Brent Love, Barbara Yu, John Bilicska, and Jason Paisley. Assistance from the flight and ground crew of the NCAR RAF C-130 facility under extreme weather conditions was very much appreciated. Thanks to Anthony Wimmers and Jennie Moody of the University of Virginia for computing the back-trajectories used in this study and to Jack Dibb, Isobel Simpson, Aaron Swanson, and two anonymous reviewers for valued manuscript comments. UCI participation in TOPSE was supported by a grant from NSF OPP.

References

Allen, D., J. E. Dibb, K. Pickering, and B. Ridley, An estimate of the stratospheric input into the troposphere during TOPSE using ^{7}Be measurements and model simulations, *J. Geophys. Res.*, doi:10.1029/2001JD001428, in press, 2002 [printed *108*(D4), 2003].

Anderson, B. E., J. E. Collins Jr., G. W. Sachse, G. W. Whiting, D. R. Blake, and F. S. Rowland, AASE-II observations of trace carbon species distributions in the mid to upper troposphere, *Geophys. Res. Lett.*, *20*, 2539–2542, 1993.

Atherton, C., Organic nitrates in remote marine environments: Evidence for long-range transport, *Geophys. Res. Lett.*, *16*, 1289–1292, 1989.

Atkinson, R., S. M. Aschmann, W. P. L. Carter, A. M. Winer, and J. N. Pitts, Alkyl nitrate formation from the NOx-air photooxidations of C_2–C_8 n-alkanes, *J. Phys. Chem.*, *86*, 4563–4569, 1982.

Atkinson, R., D. L. Baulach, R. A. Cox, R. F. Hampson, J. A. Kerr, and J. Troe, Evaluated kinetic and photochemical data for atmospheric chemistry, Supplement IV, *J. Phys. Chem. Ref. Data*, *21*, 1125, 1992.

Atlas, E., W. Pollock, J. Greenberg, L. Heidt, and A. M. Thompson, Alkyl nitrates, nonmethane hydrocarbons, and halocarbon gases over the equatorial Pacific Ocean during Saga-3, *J. Geophys. Res.*, *98*, 16,933–16,947, 1993.

Atlas, E., F. Flocke, S. Schauffler, V. Stroud, D. Blake, and F. S. Rowland, Evidence for marine sources of atmospheric alkyl nitrates: Measurements over the tropical Pacific Ocean during PEM-Tropics, *Eos Trans. AGU*, *78*(46), Fall Meet. Suppl., F115, 1997.

Beine, H. J., D. A. Jaffe, D. R. Blake, E. Atlas, and J. Harris, Measurements of PAN, alkyl nitrates, ozone and hydrocarbons during spring in interior Alaska, *J. Geophys. Res.*, *101*, 12,613–12,619, 1996.

Bertman, S. B., et al., Evolution of alkyl nitrates with air mass age, *J. Geophys. Res.*, *100*, 22,805–22,813, 1995.

Blake, D. R., and F. S. Rowland, Global atmospheric concentrations and source strength of ethane, *Nature*, *321*, 231–233, 1986.

Blake, D. R., and F. S. Rowland, Urban leakage of liquefied petroleum gas and its impact on Mexico City air quality, *Science*, *269*, 953–956, 1995.

Blake, D. R., D. F. Hurst, T. W. Smith Jr., W. J. Whipple, T.-Y. Chen, N. J. Blake, and F. S. Rowland, Summertime measurements of selected nonmethane hydrocarbons in the Arctic and subarctic during the 1988 Arctic Boundary Layer Expedition (ABLE-3A), *J. Geophys. Res.*, *97*, 16,559–16,588, 1992.

Blake, D. R., T. W. Smith Jr., T. Y. Chen, W. J. Whipple, and F. S. Rowland, Effects of biomass burning on summertime nonmethane hydrocarbon concentrations in the Canadian wetlands, *J. Geophys. Res.*, *99*, 1699–1719, 1994.

Blake, D. R., T. Y. Chen, T. W. Smith, and C. J. L. Wang, Three-dimensional distribution of nonmethane hydrocarbons and halocarbons over the northwestern Pacific during the 1991 Pacific Exploratory Mission, *J. Geophys. Res.*, *101*, 100–111, 1996.

Blake, N. J., D. R. Blake, T. Y. Chen, J. E. Collins Jr., G. W. Sachse, B. E. Anderson, and F. S. Rowland, Distribution and seasonality of selected hydrocarbons and halocarbons over the Western Pacific basin during PEM-West A and PEM-West B, *J. Geophys. Res.*, *102*, 28,315–28,331, 1997.

Blake, N. J., et al., Aircraft measurements of the latitudinal, vertical, and seasonal variations of NMHCs, methyl nitrate, methyl halides, and DMS during the First Aerosol Characterization Experiment (ACE 1), *J. Geophys. Res.*, *104*, 21,803–21,817, 1999.

Blake, N. J., D. R. Blake, A. L. Swanson, E. Atlas, F. Flocke, and F. S. Rowland, Latitudinal, vertical, and seasonal variations of C_1–C_4 alkyl nitrates in the troposphere over the Pacific Ocean during PEM-Tropics A and B: Oceanic and continental sources, *J. Geophys. Res.*, doi:10.1029/2001JD001444, in press, 2002 [printed *108*(D4), 2003].

Browell, E. V., et al., Ozone, aerosol, potential vorticity, and trace gas trends observed at high latitudes over North America from February to May 2000, *J. Geophys. Res.*, doi:10.1029/2001JD001390, in press, 2002 [printed *108*(D4), 2003].

Chin, M., D. J. Jacob, J. W. Munger, D. D. Parrish, and B. G. Doddridge, Relationship of ozone and carbon monoxide over North America, *J. Geophys. Res.*, *99*, 14,565–14,573, 1994.

Clemitshaw, K. C., J. Williams, O. V. Rattigan, D. E. Shallcross, K. S. Law, and R. A. Cox, Gas-phase ultraviolet absorption cross-sections and atmospheric lifetimes of several C_2–C_5 alkyl nitrates, *J. Photochem. Photobiol., A Chem.*, *102*, 117–126, 1997.

Colman, J. J., A. L. Swanson, S. Meinardi, B. C. Sive, D. R. Blake, and F. S. Rowland, Description of the analysis of a wide range of volatile organic compounds in whole air samples collected during PEM-Tropics A and B, *Anal. Chem.*, *73*, 3723–3731, 2001.

Crutzen, P. J., *Atmospheric Chemistry: The Atmospheric Sciences: National Objectives for the 1980's*, NRC, Washington, D. C., 1980.

Crutzen, P. J., and M. O. Andreae, Biomass burning in the tropics: Impact on atmospheric chemistry and biogeochemical cycles, *Science*, *250*, 1669–1678, 1990.

Darnall, K. R., W. P. L. Carter, A. M. Winer, A. C. Lloyd, and J. N. Pitts Jr., Importance of RO_2 + NO in alkyl nitrate formation from C_4–C_6 alkane photooxidations under simulated atmospheric conditions, *J. Phys. Chem.*, *80*, 1948–1950, 1976.

Dibb, J. E., R. W. Talbot, E. Scheuer, G. Seid, L. DeBell, B. Lefer, and B. Ridley, Stratospheric influence on the northern North American free

troposphere during TOPSE: Be-7 as a stratospheric tracer, *J. Geophys. Res.*, *107*, doi:10.1029/2001JD001347 in press, 2002.

Ehhalt, D. H., J. Rudolph, F. Meixner, and U. Schmidt, Measurements of selected C_2-C_5 hydrocarbons in the background troposphere: Vertical and latitudinal variations, *J. Atmos. Chem.*, *3*, 29, 1985.

Ehhalt, D. H., U. Schmidt, R. Zander, P. Demoulin, and C. Rinsland, Seasonal cycle and secular trend of the total column abundance of ethane above the Jungfraujoch, *J. Geophys. Res.*, *96*, 4985–4994, 1991.

Fischer, R. G., J. Kastler, and K. Ballschmiter, Levels and pattern of alkyl nitrates, multifunctional alkyl nitrates, and halocarbons in the air over the Atlantic Ocean, *J. Geophys. Res.*, *105*, 14,473–14,494, 2000.

Flocke, F., A. VolzThomas, H. J. Buers, W. Patz, H. J. Garthe, and D. Kley, Long-term measurements of alkyl nitrates in southern Germany, 1, General behavior and seasonal and diurnal variation, *J. Geophys. Res.*, *103*, 5729–5746, 1998.

Fried, A., et al., Tunable diode laser measurements of formaldehyde during the TOPSE 2000 study: Distributions, trends, and model comparisons, *J. Geophys. Res.*, doi:10.1029/2002JD002208, in press, 2002 [printed *108*(D4), 2003].

Goldstein, A. H., S. C. Wofsy, and C. M. Spivakovsky, Seasonal variations of nonmethane hydrocarbons in rural New England: Constraints on OH concentrations in northern midlatitudes, *J. Geophys. Res.*, *100*, 21,023–21,033, 1995.

Gupta, M. L., R. J. Cicerone, D. R. Blake, F. S. Rowland, and I. S. A. Isaksen, Global atmospheric concentrations and source strengths of light hydrocarbons and tetrachloroethene, *J. Geophys. Res.*, *103*, 28,219–28,235, 1998.

Hagerman, L. M., V. P. Aneja, and W. A. Lonneman, Characterization of non-methane hydrocarbons in the rural southeast United States, *Atmos. Environ.*, *31*, 4017–4038, 1997.

Hov, O., S. A. Penkett, I. S. A. Isaksen, and A. Semb, Organic gases in the Norwegian Arctic, *Geophys. Res. Lett.*, *11*, 425–428, 1984.

Hov, O., N. Schmidbauer, and M. Oehme, C_2-C_5 hydrocarbons in rural south Norway, *Atmos. Environ., Part A*, *25*, 1981–1999, 1991.

Hurst, D. F., Seasonal variations in the latitudinal distribution of tropospheric carbon monoxide, 1986–1988, dissertation, Univ. of Calif., Irvine, 1990.

Jobson, B. T., Z. Wu, H. Niki, and L. A. Barrie, Seasonal trends of isoprene, C_2-C_5 alkanes, and acetylene at a boreal site in Canada, *J. Geophys. Res.*, *99*, 1589–1599, 1994a.

Jobson, B. T., H. Niki, Y. Yokouchi, J. Bottenheim, F. Hopper, and R. Leaitch, Measurements of C_2-C_6 hydrocarbons during the Polar Sunrise 1992 Experiment: Evidence for Cl atom and Br atom chemistry, *J. Geophys. Res.*, *99*, 25,355–25,368, 1994b.

Kahl, J. D. W., D. A. Martinez, H. Kuhns, C. I. Davidson, J. L. Jaffrezo, and J. M. Harris, Air mass trajectories to Summit, Greenland: A 44-year climatology and some episodic events, *J. Geophys. Res.*, *102*, 26,861–26,875, 1997.

Lightman, P., A. S. Kallend, A. R. W. Marsh, B. M. R. Jones, and S. A. Penkett, Seasonal variation of hydrocarbons in the free troposphere at mid latitudes, *Tellus, Ser. B*, *42*, 408–422, 1990.

Lopez, J. d. P., *Seasonality and Global Growth Trends of Carbon Monoxide During 1995–2001*, Univ. of Calif., Irvine, Irvine, 2002.

Mckeen, S. A., and S. C. Liu, Hydrocarbon ratios and photochemical history of air masses, *Geophys. Res. Lett.*, *20*, 2363–2366, 1993.

McKeen, S. A., S. C. Liu, E.-Y. Hsie, X. Lin, J. D. Bradshaw, S. Smyth, G. L. Gregory, and D. R. Blake, Hydrocarbon ratios during PEM-West A: A model perspective, *J. Geophys. Res.*, *101*, 2087–2109, 1996.

Mauldin, L., et al., Hydroxyl radical measurements during TOPSE, in press, 2002.

Muthuramu, K., P. B. Shepson, J. Bottenheim, B. T. Jobson, H. Niki, and K. G. Anlauf, Relationships between organic nitrates and surface ozone destruction during Polar Sunrise Experiment 1992, *J. Geophys. Res.*, *99*, 25,369–25,379, 1994.

Penkett, S. A., N. J. Blake, P. Lightman, A. R. W. Marsh, P. Anwyl, and G. Butcher, The seasonal variation of non-methane hydrocarbons in the free troposphere over the North Atlantic Ocean: Possible evidence for extensive reaction of hydrocarbons with the nitrate radical, *J. Geophys. Res.*, *98*, 2865–2885, 1993.

Rasmussen, R. A., M. A. K. Khalil, and J. S. Chang, Atmospheric trace gases over China, *Environ. Sci. Technol.*, *16*, 124, 1982.

Ridley, B. A., et al., Aircraft measurements made during the spring maximum of ozone over Hawaii: Peroxides, CO, O_3, NO_y, condensation nuclei, selected hydrocarbons, halocarbons, and alkyl nitrates between 0.5 and 9 km, *J. Geophys. Res.*, *102*, 18,935–18,961, 1997.

Ridley, B. A., et al., Ozone depletion events observed in the high latitude surface layer during the TOPSE aircraft program, *J. Geophys. Res.*, 2002 [printed *108*(D4), 2003].

Roberts, J. M., The atmospheric chemistry of organic nitrates, *Atmos. Environ.*, *24*, 243–287, 1990.

Roberts, M., et al., Relationships between PAN and ozone at sites in eastern North America, *J. Geophys. Res.*, *100*, 22,821–22,830, 1995.

Roberts, J. M., S. B. Bertman, D. D. Parrish, F. C. Fehsenfeld, B. T. Jobson, and H. Niki, Measurement of alkyl nitrates at Chebogue Point, Nova Scotia during the 1993 North Atlantic Regional Experiment (NARE) intensive, *J. Geophys. Res.*, *103*, 13,569–13,580, 1998.

Rudolph, J., and F. J. Johnen, Measurements of light atmospheric hydrocarbons over the Atlantic in regions of low biological activity, *J. Geophys. Res.*, *95*, 20,583–20,591, 1990.

Sexton, K., and H. Westberg, Ambient air measurements of petroleum refinery emissions, *J. Air Pollut. Control Assoc.*, *29*, 1149–1152, 1979.

Sharma, U. K., Y. Kajii, and H. Akimoto, Seasonal variation of C_2-C_6 NMHCs at Happo, a remote site in Japan, *Atmos. Environ.*, *34*, 4447–4458, 2000.

Singh, H. B., and L. J. Salas, Measurements of selected light hydrocarbons over the Pacific Ocean: Latitudinal and seasonal variation, *Geophys. Res. Lett.*, *9*, 842–845, 1982.

Singh, H. B., W. V. Viezee, and L. J. Salas, Measurements of selected C_2-C_5 hydrocarbons in the troposphere: Latitudinal, vertical, and temporal variations, *J. Geophys. Res.*, *93*, 15,861, 1988.

Sive, B. C., Analytical methods and estimated hydroxyl radical concentrations, Ph.D. thesis, Univ. of Calif., Irvine, Irvine, 1998.

Smyth, S. B., et al., Factors influencing the upper free tropospheric distribution of reactive nitrogen over the South Atlantic during the TRACE-A experiment, *J. Geophys. Res.*, *101*, 24,165–24,186, 1996.

Spivakovsky, C. M., et al., Three-dimensional climatological distribution of tropospheric OH: Update and evaluation, *J. Geophys. Res.*, *105*, 8931–8980, 2000.

Wang, C. J.-L., D. R. Blake, and F. S. Rowland, Seasonal variations in the atmospheric distribution of a reactive chlorine compound, tetrachloroethene ($CCl_2 = CCl_2$), *Geophys. Res. Lett.*, *22*, 1097–1100, 1995.

Wang, Y., et al., Springtime photochemistry at northern mid and high latitudes, *J. Geophys. Res.*, doi:10.1029/2002JD00227, in press, 2002 [printed *108*(D4), 2003].

Wingenter, O. W., M. K. Kubo, N. J. Blake, T. W. Smith Jr., D. R. Blake, and F. Sherwood Rowland, Hydrocarbon and halocarbon measurements as photochemical and dynamical indicators of atmospheric hydroxyl, atomic chlorine, and vertical mixing obtained during Lagrangian flights, *J. Geophys. Res.*, *101*, 4331–4340, 1996.

Wingenter, O. W., D. R. Blake, N. J. Blake, B. C. Sive, and F. S. Rowland, Tropospheric hydroxyl and atomic chlorine concentrations, and mixing time scales determined from hydrocarbon and halocarbon measurements made over the Southern Ocean, *J. Geophys. Res.*, *104*, 21,819–21,828, 1999.

E. L. Atlas, F. Flocke, and B. A. Ridley, Atmospheric Chemistry Division, National Center for Atmospheric Research (NCAR), 1850 Table Mesa Drive, Boulder, CO 80307, USA.

D. R. Blake, N. J. Blake, A. S. Katzenstein, S. Meinardi, and F. S. Rowland, Department of Chemistry, University of California, Irvine, Irvine, CA 92697-2025, USA. (nblake@uci.edu)

O. W. Wingenter, Department of Chemistry, New Mexico Institute of Mining and Technology, Socorro, NM 87801-4750, USA.

B. C. Sive, Climate Change Research Center, Institute for the Study of Earth, Oceans, and Space, University of New Hampshire, Durham, NH 03824, USA.